

## Critical dynamics below the percolation threshold

This article has been downloaded from IOPscience. Please scroll down to see the full text article.

1993 J. Phys. A: Math. Gen. 26 L1211

(<http://iopscience.iop.org/0305-4470/26/23/004>)

View [the table of contents for this issue](#), or go to the [journal homepage](#) for more

Download details:

IP Address: 171.66.16.68

The article was downloaded on 01/06/2010 at 20:09

Please note that [terms and conditions apply](#).

## LETTER TO THE EDITOR

# Critical dynamics below the percolation threshold

S Jain<sup>†</sup> and E J S Lage<sup>‡</sup>

<sup>†</sup> School of Mathematics and Computing, Faculty of Science and Technology, University of Derby, Kedleston Road, Derby DE22 1GB, UK

<sup>‡</sup> Centro de Física da Universidade de Porto, Faculdade de Ciências, Praça Gomes Teixeira, 4000 Porto, Portugal

Received 4 October 1993

**Abstract.** The critical dynamics of the diluted two-dimensional Ising model below the percolation threshold is studied. The dynamics exhibits a crossover from a concentration-dependent behaviour for  $\xi_T \gg \xi_p$  to a percolating lattice type behaviour for  $\xi_T \ll \xi_p$ , where  $\xi_T$  and  $\xi_p$  are the thermal and percolation correlation lengths, respectively. As a consequence, the dynamical exponents  $A$  and  $B$  are shown to be the limits of dynamical functions  $A(x)$  and  $B(x)$ , respectively; here,  $x = \ln \xi_p / \ln \xi_T$ . Extensive Monte Carlo simulations support our predictions.

The critical dynamics of disordered spin systems have attracted considerable interest in recent years. It is now fairly well established [1-9] that conventional dynamic scaling [10] breaks down for diluted spin systems at the percolation threshold. According to conventional dynamic scaling, the average time,  $\tau_{AV}(T)$ , scales as

$$\ln \tau_{AV}(T) \sim Z \ln \xi_T \quad (1)$$

where  $\xi_T$  is the thermal correlation length and  $Z$  is a dynamic critical exponent. At  $p = p_c$ , the percolation threshold, it is found the  $Z$  is in fact a temperature-dependent function

$$Z(T) = A(\ln \xi_T) + B \quad (2)$$

where  $A$  and  $B$  are two new dynamical exponents. Both analytic [2-4, 7, 8] and computational [5, 6, 9] results confirm the new dynamics for Ising and Potts models at the percolation threshold; estimates of  $A$  and  $B$  for various two-dimensional models may be found in Jain [9]. Very recently, critical crossover phenomena has been reported by Heuer [11] who investigated site-disordered Ising systems over a large range of dilution above the percolation threshold ( $0.6 \leq p \leq 1.0$ ).

In this letter we study the critical behaviour of systems *below* the percolation threshold ( $p < p_c$ ). We present both analytical and computational results. By applying the arguments of Harris and Stinchcombe [2], we shall show that for  $p < p_c$  we have to introduce dynamical exponents which take the form of scaling functions,  $A$  and  $B$  being retrieved in appropriate limits. Furthermore, we also report the results of extensive Monte Carlo simulations of the two-dimensional Ising model on a square lattice with bond-dilution which support our analytical predictions. A preliminary account of this work was presented at the Vth Rencontres de Blois on 'Chaos and Complexity' [12].

The Hamiltonian is given by

$$H = - \sum_{\langle ij \rangle} J_{ij} S_i S_j \quad (3)$$

where Ising spins  $S_i = \pm 1$  are situated on every lattice site, the sum runs over nearest neighbours only and the quenched ferromagnetic couplings are selected according to

$$P(J_{ij}) = (1-p)\delta(J_{ij}) + p\delta(J_{ij}-1) \quad (4)$$

$p$  being the bond concentration. Boltzmann's constant and the nearest-neighbour interaction are both set to unity. The pure system has a second-order phase transition at  $T_c(p=1) = 2/\ln(1+2^{1/2})$  and, of course,  $T_c(p=p_c=1/2) = 0$ .

The correlation length,  $\xi(T, p)$ , is given by [11]

$$\xi^{-1}(T, p) = \xi_T^{-1}(T, p_c) + \xi_p^{-1}(0, p) \quad (5)$$

where  $\xi_T$  and  $\xi_p$  are the thermal and percolation correlation lengths, respectively. At  $p=p_c$  the correlation length is given by just the thermal correlation length because the percolation correlation length is infinite. Below  $p_c$ , however, we have to take *both* correlation lengths into consideration; further, we have [13]

$$\xi_T = \xi_0 e^{2\nu_T/T} \quad (6)$$

where [6]  $\xi_0 = 0.22 \pm 0.01$  and

$$\xi_p \sim (p_c - p)^{-\nu_p}. \quad (7)$$

The cross-over exponent [14] is predicted to be 1 and, as a consequence, we can identify [6, 15]  $\nu_T = \nu_p 4/3$ .

We consider Metropolis dynamics [16] in which the spins are updated according to

$$W(S_i \rightarrow -S_i) = \min\{1, \exp(-\Delta E/T)\} \quad (8)$$

where  $\Delta E$  is the energy change involved.

We adopt the real-space renormalization group technique of Harris and Stinchcombe [2]. In this approach one considers a honeycomb lattice with configurational disorder and replaces it with a similar lattice dilated by a scale factor  $b=2$ . ([2] should be consulted for further technical details.) After  $n$  iterations, the average relaxation time for a domain wall to traverse a renormalized bond is given by [2]

$$T_{AV} \sim \left[ \frac{\xi_T^n}{b^{n(n-1)/2}} \right]^{1/\nu_T}. \quad (9)$$

If  $\xi_T \ll \xi_p$ , the iterations stop at  $b^n \sim \xi_T$  and we obtain

$$\ln \tau_{AV} = A(\ln \xi_T)^2 + B(\ln \xi_T) \quad (10)$$

with  $A = 1/2\nu_T \ln b$ , and  $B = 1/2\nu_T$  (+ corrections). Equation (10) is, of course, identical to the form obtained at  $p_c$  (see equations (1) and (2)).

If  $\xi_T \gg \xi_p$ , the iterations stop at  $b^n \sim \xi_p$  and we get instead of equation (10) that

$$\ln \tau_{AV} = \frac{1}{2\nu_T \ln b} [2 \ln \xi_p \ln \xi_T - (\ln \xi_p)^2 + \ln \xi_p \ln b]. \quad (11)$$

Both limits,  $\xi_T \ll \xi_p$  and  $\xi_T \gg \xi_p$ , can be obtained from

$$\ln \tau_{AV} = A(x)(\ln \xi_T)^2 + B(x)(\ln \xi_T) \quad (12)$$

where  $x = \ln \xi_p / \ln \xi_T$  and the functional dependence of  $A$  and  $B$  has been indicated explicitly. The two scaling functions,  $A(x)$  and  $B(x)$ , are such that

$$A(x) = \begin{cases} A & \text{for } x \rightarrow \infty \\ \frac{2x - x^2}{2v_T \ln b} & \text{for } x \ll 1 \end{cases} \quad (13)$$

and

$$B(x) = \begin{cases} B & \text{for } x \rightarrow \infty \\ \frac{x}{2v_T} & \text{for } x \ll 1. \end{cases} \quad (14)$$

We now discuss the results of Monte Carlo simulations of the bond-diluted two-dimensional Ising model on a square  $64 \times 64$  lattice.

For any given  $p$  and temperature,  $T$ , the nearest-neighbour interactions are chosen according to equation (4). Periodic boundary conditions are imposed throughout this work. The spins are all pointing up at the start and we perform a conventional Monte Carlo simulation [17] of the system using the transition probability given in equation (8). The data presented here were collected over the ranges  $0.25 \leq T \leq 1.2$  and  $0.1 \leq p \leq 0.3$ , and have been averaged over many samples (50–10 000).

The key quantity studied in the simulations is  $\tau_{AV}$ , the average relaxation time, which is given by

$$\tau_{AV} = \int_0^{\infty} C(t) dt \quad (15)$$

and here  $C(t) = N^{-1} \sum_i S_i(t_0) S_i(t_0 + t)$ , where  $t_0$  is an initial time,  $t > t_0$  and, in this particular situation,  $N = 4096$ . We choose  $t_0$  so that  $t_0 \geq \tau_0$ , the equilibration time of the system.

In figure 1 we show a log-log plot of  $\tau_{AV}$  against  $\xi_T$  for various values of bond concentrations over the range ( $0.7 \leq \ln \xi_T \leq 9.2$ ); note that the thermal correlation length has been determined from equation (6). Throughout our simulations we have  $\min(\xi_T, \xi_p) \ll$  the linear size of the lattice. Consequently, our results are not expected to be influenced by finite-size effects.

Clearly, for each value of  $p$ , the divergence of  $\ln \tau_{AV}$  falls into two regimes: an initial nonlinear divergence and an apparently linear divergence, providing  $\xi_T$  is sufficiently large. To see if the initial divergence is indeed quadratic as predicted by equation (10), we show a magnified plot of the data for  $0.7 \leq \ln \xi_T \leq 2.3$  in figure 2. (For clarity, we have omitted the data for  $p = 0.3$ ). The best overall quadratic fit in each case is also displayed. It should be remembered that whereas equation (10) is only valid for  $\xi_T \ll \xi_p$ , the data shown in figure 2 also include those for  $\xi_T \sim \xi_p$ . As a consequence, one should not be too surprised by the deviations from the quadratic fits, especially for moderately large bond concentrations. Further, it is clear from equation (12) that we expect the quadratics in question to have coefficients  $A(x)$  and  $B(x)$  which vary with the ratio  $\ln \xi_p / \ln \xi_T (= x)$ . In figure 3 we plot the coefficients of the quadratic

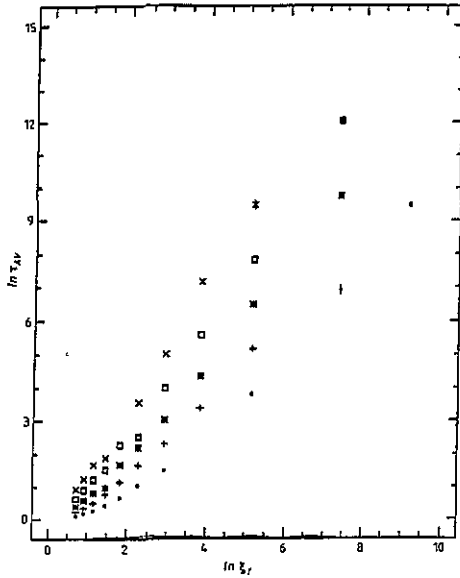


Figure 1. A plot of  $\ln \tau_{AV}$  against  $\ln \xi_T$  for various bond concentrations  $p$ :  $\bullet$ ,  $p=0.1$ ;  $+$ ,  $p=0.15$ ;  $*$ ,  $p=0.2$ ;  $\square$ ,  $p=0.25$ ;  $\times$ ,  $p=0.3$ .

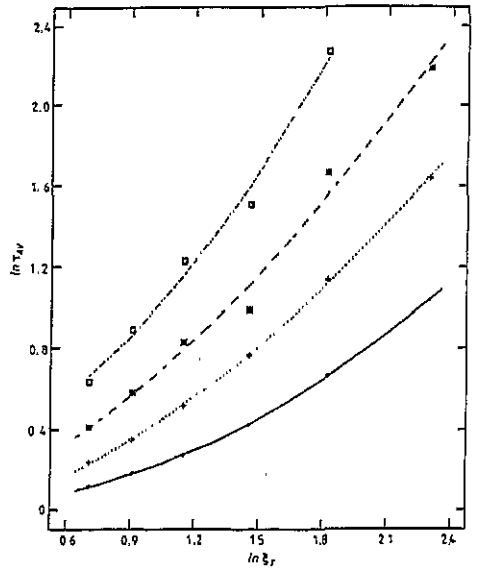


Figure 2. A magnified plot of  $\ln \tau_{AV}$  against  $\ln \xi_T$  for  $0.7 \leq \ln \xi_T \leq 2.3$ . The best quadratic fit in each case is also shown.  $\bullet$ ,  $p=0.1$ ;  $+$ ,  $p=0.15$ ;  $*$ ,  $p=0.2$ ;  $\square$ ,  $p=0.25$ .

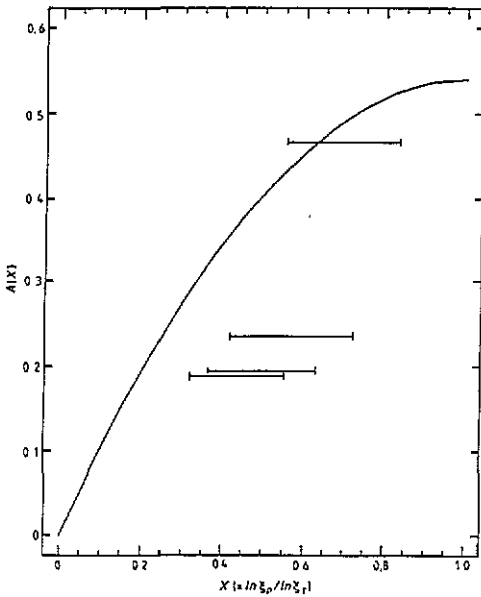


Figure 3. A plot of  $A(x)$  against  $x$ . Also shown are the values of the coefficients of the quadratic terms for the fits shown in figure 2. (See text.)

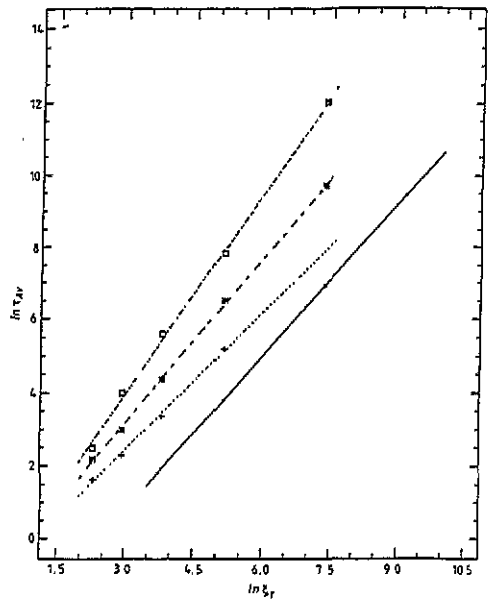


Figure 4. A magnified plot of  $\ln \tau_{AV}$  against  $\ln \xi_T$  for  $2.4 \leq \ln \xi_T \leq 9.2$ . The best linear fit in each case is also shown.  $\bullet$ ,  $p=0.1$ ;  $+$ ,  $p=0.15$ ;  $*$ ,  $p=0.2$ ;  $\square$ ,  $p=0.25$ .

**Table 1.** Values of the gradients of the linear fits shown in figure 4 and the corresponding term in equation (11). (See text.)

$P$	0.1	0.15	0.2	0.25
Gradient	1.41	1.24	1.50	1.84
$\ln \xi_p / v_T \ln b$	1.32	1.51	1.74	2.00

**Table 2.** Values of  $x(p)$  at the crossover as determined from figure 1.

$p$	0.1	0.15	0.2	0.25	0.3
$x^c(p)$	0.24	0.30	0.31	0.40	0.50

terms against  $x$  for the fits shown in figure 2, the range of  $x$  values in each case being determined by the range over which each fit is valid. Also shown in figure 3 is the predicted form of  $A(x)$  as determined by equation (13). Clearly, our numerical values are in good qualitative agreement with the theory. The quantitative discrepancy can be understood by the reservations outlined above.

In the other regime, namely  $\xi_T \gg \xi_p$ , we expect equation (11) to hold. In figure 4 we show a magnified plot of the data for  $2.4 \leq \ln \xi_T \leq 9.2$ . Here the divergence of  $\ln \tau_{AV}$  is evidently linear as predicted. The line of best fit in each case is also shown and the gradients are given in table 1. These should be compared with the theoretical values which are also given in table 1.

The crossover between the two regimes occurs at  $x^c(p)$  (where  $x = \ln \xi_p / \ln \xi_T$ ), which, as determined from figure 1, would appear to be a monotonically increasing function of  $p$  (see table 2).

To conclude, we have studied the critical dynamics of the diluted two-dimensional Ising model below the percolation threshold. We have shown that there is a crossover at  $x^c(p)$  from a concentration-dependent behaviour for  $\xi_T \gg \xi_p$  to a percolating lattice type behaviour for  $\xi_T \ll \xi_p$ ;  $x^c(p)$  would appear to be a monotonically increasing function of  $p$ . Furthermore, the dynamical exponents  $A$  and  $B$  are actually the limits of dynamical functions  $A(x)$  and  $B(x)$ , respectively. Our numerical results are consistent with the theory.

The simulations were performed on the AMT-DAP at Queen Mary and Westfield College (London University). The Science and Engineering Research Council of Great Britain is gratefully acknowledged.

## References

- [1] Henley C L 1985 *Phys. Rev. Lett.* **54** 2030
- [2] Harris C K and Stinchcombe R B 1986 *Phys. Rev. Lett.* **56** 869
- [3] Stinchcombe R B 1985 *Scaling Phenomena in Disordered Systems* ed R Pynn and A Skjeltorp (New York: Plenum)
- [4] Lage E J S 1986 *J. Phys. C: Solid State Phys.* **19** L91
- [5] Rammal R and Benoit A 1985 *J. Physique Lett.* **46** L667; 1985 *Phys. Rev. Lett.* **55** 649  
Chowdhury D and Stauffer D 1986 *J. Phys. A: Math. Gen.* **19** L19  
Pytte E 1986 *Phys. Rev. B* **34** 2060

- [6] Jain S 1986 *J. Phys. A: Math. Gen.* **19** L57, L667
- [7] Jain S, Lage E J S and Stinchcombe R B 1986 *J. Phys. C: Solid State Phys.* **19** L805
- [8] Nunes da Silva J M and Lage E J S 1987 *J. Phys A: Math. Gen.* **20** 2655; 1987 *J. Phys C: Solid State Phys.* **20** L275
- [9] Jain S 1988 *J. Phys. A: Math. Gen.* **21** L179
- [10] Hohenberg P C and Halperin B I 1977 *Rev. Mod. Phys.* **49** 435
- [11] Heuer H-O 1993 *J. Phys. A: Math. Gen.* **26** L333
- [12] Jain S 1993 *Chaos and Complexity (Proc. Vth Rencontres de Blois)* to be published
- [13] Stinchcombe R B 1983 *Phase Transitions and Critical Phenomena* vol 7, ed C Domb and J L Lebowitz (New York: Academic) p 151
- [14] Stephen M J and Grest G S 1977 *Phys. Rev. Lett.* **38** 567  
Coniglio A 1981 *Phys. Rev. Lett.* **46** 250
- [15] den Nijs M P 1979 *J. Phys. A: Math. Gen.* **12** 1857  
Neinhuis B, Riedel E K and Schick M 1980 *J. Phys. A: Math. Gen.* **13** L189
- [16] Metropolis N, Rosenbluth A W, Rosenbluth M H, Teller A H and Teller E 1953 *J. Chem. Phys.* **21** 1087
- [17] Jain S 1992 *Monte Carlo Simulations of Disordered Systems* (Singapore: World Scientific)